$$\mathcal{U}_{jk} = E\left(\frac{v_{j,k+1} - v_{j,k}}{b}\right)^2 \Omega_j b \qquad \text{(IV5)}$$

and the kinetic energy, associated with axial displacement:

$$\mathcal{T}_{jk} = \Omega_j \rho_s b \int_0^1 \left[v_{j,k+1}(1-\eta) + v_{j,k}\,\eta\right]^2 d\eta \qquad \text{(IV6)}$$

3. *Rigid Motion*
For rigid motion, we only have to compute kinetic energy associated with **P**.

$$\mathcal{T} = ab \int_0^1 d\xi \int_0^1 d\eta\,\mu(\xi,\eta)[\mathbf{P}_A(1-\eta) + \mathbf{P}_B(\eta)]^2 \qquad \text{(IV7)}$$

For μ we include, as already said, panels, and stringers mass. This is $6 \cdot 6$ matrix.

4. *Assembly*
Clearly, each of the above matrices must be assembled in the matrices appearing in Equation (27). Assembly is made through a routine procedure.

REFERENCES

1. Santini, P., F. Betti, P. Gasbarri and A. Rossi. 1993. "Actively Damped Piezoelectric Composite Wing," *Damping 93,* 24–26 Feb., San Francisco, CA.
2. Santini, P., P. Gasbarri, M. Altobelli and A. Rossi. 1994. "A Comparative Overview of Strain Actuated Surface Design," *Fifth International Conference on Adaptive Structures.* Sendai, Japan 5–7, December.
3. Gasbarri, P., F. Betti, F. Persiani and G. M. Saggiani. 1994. "Static Aeroelastic Control of an Adaptive Wing," *ICAS 94. Congress of the International Council of the Aeronautical Science,* Anaheim, 18–23 September.
4. Santini, P. and A. Sermoneta. 1994. "Structural Analysis of Multistringer Panel," Z. Flugwissenschaften und Weltraumforschung. Vol. 18, Springer Verlag.
5. Santini, P. and A. Sermoneta. 1995. "Structural Analysis of a Composite Wingbox," Z. Flugwissenschaften und Weltraumforschung. Vol. 19, Springer Verlag.
6. Santini, P. 1986. "Construzioni Aeronautiche," E.S.A.
7. Karpel, M. and E. Presente. "Structural Dynamic Loads in Response to Impulsive Excitation," *Journal of Aircraft,* 32:4.

Prediction of Creep Properties of Laminated Composites from Matrix Creep Data

J. S. HARRIS AND E. J. BARBERO*
West Virginia University
Morgantown, WV 26506-6106

ABSTRACT: A new model to predict the creep response of laminated composite materials is presented. The correspondence principle is used to perform the micro- and macro-mechanics analysis in the Laplace domain. A new set of micromechanical formulas are used, which are accurate without the use of empirical correction factors. A macro-mechanical model is developed, which includes provisions for modeling materials with randomly oriented reinforcement. Experimental data for the neat vinyl ester resin and various laminates is presented. The theoretical model accurately predicts the experimental creep response of polymer matrix composites considered in this work.

1. INTRODUCTION

POLYMER MATRIX COMPOSITES (PMC) display important viscoelastic behavior, which is sensitive to environmental effects (temperature, humidity, radiation, etc.). The general constitutive relations between applied stress and strain for viscoelastic response are described by Schapery [19,20]. Short and long term creep effects have been experimentally studied, but very few micro-mechanical and macro-mechanical models have been developed to predict creep of laminated composite materials from constituent properties. On the other hand, many micro-mechanical models have been developed to describe the elastic behavior of unidirectional composite materials. Such models include approximate equations such as the rule of mixtures formulas [12], formulas using correction factors such as the Tsai-Halpin formulas [4], and asymptotically exact formulas [17], among many others.

The correspondence principle [3] offers a powerful tool for modeling linearly viscoelastic materials; that is, when the viscoelastic behavior can be assumed to be

*Author to whom correspondence should be addressed.

0731-6844/98/04 0361–19 $10.00/0

independent of the stress level. Using the correspondence principle, most analytical tools developed for elastic materials can be used by taking a Laplace transform. This excludes iterative techniques (e.g., the self consistent method) and formulas containing empirical factors because the dependence of empirical factors as a function of time is unknown. In structural design, the sizing of members, and thus the level of stress is determined to satisfy requirements such as maximum deflections, fatigue limits, notched strength, compression after impact, etc. Therefore, the structure is likely to operate in a relatively narrow range of stress values. In this case, the material can be assumed to be linearly viscoelastic within the operating range of stress.

The creep behavior of any linearly viscoelastic material can be represented by empirical models such as the power law, Maxwell, Voigt, and Maxwell-Voigt models [8], etc. These empirical models simply represent a curve fit of experimental creep data. The problem with this approach is the prohibitive cost associated with creep testing of composites with various fibers and resin types, various values of fiber volume fraction, under various temperature and moisture conditions, etc. Also, several types of tests are necessary to evaluate the creep behavior in shear as well as longitudinal and transverse directions [25]. If linear viscoelasticity cannot be used, more complex models such as the Schapery nonlinear model [16] have to be used.

Previous use of micro-mechanical models include the rule of mixtures, which was used by Lee and Ueng [14] along with a numerical solution procedure for a uniaxial state of stress. The micro-mechanics method of cells proposed by Aboudi [1–3] was used by Yancey and Pindera [24] to obtain the effective elastic moduli of the composite in the Laplace domain, in terms of the constituent moduli and volume fractions. A numerical method proposed by Bellman [6] was used for the inversion of the effective moduli in the Laplace domain to the time domain. The creep properties of the matrix and the elastic properties of the fibers were back-calculated using the same model.

The present work uses a new micro-mechanics model that provides closed-form analytical formulas for all the components of the relaxation tensor while retaining the accuracy of an asymptotically exact solution. Any geometry of fibers and spatial distribution of inclusions can be modeled [17]. Furthermore, layers with random reinforcement are included in the macro-mechanical model. Original experimental data is generated to validate the model. The experimental data is based on laminated composites including continuous strand mat, unidirectional, and bi-directional stitched fabric layers. The fabrics were supplied by Brunswick Technology Inc. The composites were fabricated by Hard Core DuPont using Derakane resin supplied by Dow Chemical. Neat resin samples were tested to obtain the matrix creep properties directly, without relying on back calculation using any micro-mechanics equations. Besides being economical, this method has the advantage that various matrices can be experimentally qualified for creep response under various environmental conditions (temperature, moisture, radiation) before fabricating any composite samples. Potential does exist for relating the creep behavior of the polymer matrix to the polymer structure [9]. In this way, the present work contributes to the development of a model to predict the influence of polymer structure on the final composite properties.

Once the creep behavior (shear, longitudinal, and transverse) of the composite is known, either at the layer or laminate level, several numerical methods exist to integrate the viscoelastic equations. General laminate predictions were obtained by Dillard [7] using numerical integration in the time domain. The creep properties of each layer in the laminate were determined experimentally for the actual composite material as explained, for example, by Tuttle and Brinson [23]. Lin and Hwang [15] used the finite element method and the general constitutive equations for viscoelastic materials applied directly to the laminate. Kennedy and Wang [13] modeled individual plies in the laminate using 20-node isoparametric solid elements. An alternative method to finite elements, proposed by Zhang and Xiang [26], provides the viscoelastic response by using the viscoelastic constitutive relation given by Schapery [19]. The parameters of the constutative equations of the laminate are determined experimentally. A method proposed by Singhal and Chamis [22] uses a general power law to describe the viscoelastic response of composites with the parameters being determined experimentally for the laminate. A problem encountered with these proposed models is that they rely on experimental results of the composite. This means that an expensive experimental program needs to be completed before attempting the design of the composite.

Halpin and Sims [11] used a combined micro-mechanical and macro-mechanical approach to predict the overall creep response of unidirectional or laminated composites. They used the semi-empirical Halpin-Tsai micro-mechanics formulas [4] for an elastic material to determine the viscoelastic response of a unidirectional composite. In order to use the correspondence principle, a Laplace transform of the Halpin-Tsai equations has to be done. But, these equations contain empirical parameters which may be a function of time. Sims and Halpin back-calculated the matrix creep behavior from composite creep data assuming the empirical parameters to be independent of time.

In this paper, the micro-mechanics used does not contain any empirical parameters. While the micro-mechanics used here is asymptotically exact without requiring empirical correction factors, the formulas are still analytical expressions, thus facilitating the evaluation of their Laplace transform. Furthermore, the micro-mechanics used here accounts for the geometry of the inclusions, whether these are fibers or particles. The fibers are considered to be elastic and transversely isotropic. The matrix is assumed to be linearly viscoelastic. The model uses parameters determined experimentally from matrix creep tests, and the known elastic properties of the fibers, to determine the overall viscoelastic performance of a laminated composite.

2. MICROMECHANICS

The micro-mechanics used to describe the composite viscoelastic behavior is a closed form solution based on Fourier expansion developed by Luciano and Barbero [17] which offers a better representation of the shear and transverse properties without the need of empirical correction parameters. Using the correspondence principle for linearly viscoelastic materials, the micro-mechanics formulas developed for elastic materials can be used directly in the Laplace domain. The equations are easier to manipulate using the Carson transform (indicated by $\hat{L}$), which is related to the Laplace transform (indicated by $\tilde{L}$) by

$$\hat{L}^*[f(t)] = s\tilde{L}^*[f(t)]$$

where $f(t)$ is any function of time.

The components of the relaxation tensor in the Carson domain for a unidirectional composite with periodically arranged fibers given by [5,18]

$$\hat{L}_{11}(s) = \hat{\lambda}_0 + 2\hat{\mu}_0 - v_f \times \left[\frac{S_3^2}{\hat{\mu}_0^2} - \frac{2S_6S_3}{\hat{\mu}_0^2 g} - \frac{aS_3}{\hat{\mu}_0 c} + \frac{S_6^2 - S_7^2}{\hat{\mu}_0^2 g^2} + \frac{aS_6 + bS_7}{\hat{\mu}_0 gc} + \frac{a^2 - b^2}{4c^2}\right] \Big/ D$$

$$\hat{L}_{12}(s) = \hat{\lambda}_0 + v_f b\left[\frac{S_3}{2c\hat{\mu}_0} - \frac{S_6 - S_7}{2c\hat{\mu}_0 g} - \frac{a+b}{4c^2}\right] \Big/ D$$

$$\hat{L}_{23}(s) = \hat{\lambda}_0 + v_f\left[\frac{aS_7}{2\hat{\mu}_0 gc} - \frac{ba + b^2}{4c^2}\right] \Big/ D \tag{1}$$

$$\hat{L}_{22}(s) = \hat{\lambda}_0 + 2\hat{\mu}_0 - v_f\left[-\frac{aS_3}{2\hat{\mu}_0 c} + \frac{aS_6}{2\hat{\mu}_0 gc} + \frac{a^2 - b^2}{4c^2}\right] \Big/ D$$

$$\hat{L}_{44}(s) = \hat{\mu}_0 - v_f\left[-\frac{2S_3}{\hat{\mu}_0} + (\hat{\mu}_0 - \mu_1)^{-1} + \frac{4S_7}{\hat{\mu}_0(2 - 2v_0)}\right]^{-1}$$

$$\hat{L}_{66}(s) = \hat{\mu}_0 - v_f\left[-\frac{S_3}{\hat{\mu}_0} + (\hat{\mu}_0 - \mu_1)^{-1}\right]^{-1}$$

where

$$D = \frac{aS_3^2}{2\hat{\mu}_0^2 c} - \frac{aS_6S_3}{\hat{\mu}_0^2 gc} + \frac{a(S_6^2 - S_7^2)}{2\hat{\mu}_0^2 g^2 c} + \frac{S_3(b^2 - a^2)}{2\hat{\mu}_0 c^2} + \frac{S_6(a^2 - b^2) + S_7(ab + b^2)}{2\hat{\mu}_0 gc^2} + \frac{(a^3 - 2b^3 - 3ab^2)}{8c^3}$$

and

$$a = \mu_1 - \hat{\mu}_0 - 2\mu_1 v_0 + 2\hat{\mu}_0 v_1$$

$$b = -\hat{\mu}_0 v_0 + \mu_1 v_1 + 2\hat{\mu}_0 v_0 v_1 - 2\mu_1 v_0 v_1$$

$$c = (\hat{\mu}_0 - \mu_1)(-\hat{\mu}_0 + \mu_1 - \hat{\mu}_0 v_0 - 2\mu_1 v_0 + 2\hat{\mu}_0 v_1 + \mu_1 v_1 + 2\hat{\mu}_0 v_0 v_1 - 2\mu_1 v_0 v_1)$$

$$g = (2 - 2v_0)$$

The series S_3, S_6, S_7 represent the geometry and spatial distribution of the inclusions. For circular cylindrical fibers, they are given by [17]

$$\begin{aligned} S_3 &= 0.49247 - 0.47603v_f - 0.02748v_f^2 \\ S_6 &= 0.36844 - 0.14944v_f - 0.27152v_f^2 \\ S_7 &= 0.12346 - 0.32035v_f + 0.23517v_f^2 \end{aligned}$$

where v_f is the fiber volume fraction and the Lamé constants are given by

$$\begin{aligned} \hat{\lambda}_0 &= \frac{\hat{E}_0 v_0}{(1+v_0)(1-2v_0)} \\ \hat{\mu}_0 &= \frac{\hat{E}_0}{2(1+v_0)} \end{aligned} \tag{2}$$

where $\hat{E}_0$ and v_0 are the relaxation modulus and the Poisson ratio of the matrix, E_1 and v_1 are the elastic modulus and the Poisson ratio of the fiber. The Poisson ratio of the matrix is considered constant over time, consistently with earlier work [3]. The matrix data can be represented by any empirical model (Maxwell, Maxwell-Kelvin, Power Law, etc.)

To model a material with transverse isotropy, the following averaging procedure is used

$$\hat{C} = \frac{1}{\pi}\int_0^{\pi} [R][\hat{L}][R]^T \, d\theta \tag{3}$$

where the rotational matrix $[R]$ is the fourth-order orthogonal rotational tensor representing a rotation θ about the x_1 axis (fiber direction). After completing the integration, the tensor $\hat{C}$ is given by

$$\begin{aligned}
\hat{C}_{11} &= \hat{L}_{11} \\
\hat{C}_{12} &= \hat{L}_{12} \\
\hat{C}_{22} &= \frac{3}{4}\hat{L}_{22} + \frac{1}{4}\hat{L}_{23} + \frac{1}{2}\hat{L}_{44} \\
\hat{C}_{23} &= \frac{1}{4}\hat{L}_{22} + \frac{3}{4}\hat{L}_{23} - \frac{1}{2}\hat{L}_{44} \\
\hat{C}_{66}(t) &= \hat{L}_{66} \\
\hat{C}_{44} &= \frac{1}{4}(\hat{L}_{22} - \hat{L}_{23} + 2\hat{L}_{44})
\end{aligned} \tag{4}$$

where the new tensor is the averaged relaxation tensor for a transversely isotropic material.

3. MACROMECHANICS

A relation between the relaxation trensor $[\hat{C}]$ and the reduced relaxation matrix $[\hat{Q}]$ for a unidirectional layer can be found by applying plain stress conditions to the following constitutive equation

$$\begin{Bmatrix} \hat{\sigma}_1 \\ \hat{\sigma}_2 \\ 0 \\ 0 \\ 0 \\ \hat{\sigma}_6 \end{Bmatrix} = \begin{bmatrix} \hat{C}_{11} & \hat{C}_{12} & \hat{C}_{12} & 0 & 0 & 0 \\ & \hat{C}_{22} & \hat{C}_{23} & 0 & 0 & 0 \\ & & \hat{C}_{22} & 0 & 0 & 0 \\ & & & \hat{C}_{44} & 0 & 0 \\ & & & & \hat{C}_{66} & 0 \\ \text{sym.} & & & & & \hat{C}_{66} \end{bmatrix} \begin{Bmatrix} \hat{\varepsilon}_1 \\ \hat{\varepsilon}_2 \\ \hat{\varepsilon}_3 \\ 0 \\ 0 \\ \hat{\gamma}_6/2 \end{Bmatrix} \tag{5}$$

By expanding Equation (5), the new reduced relaxation coefficients are given by

$$\begin{aligned}
\hat{Q}_{11} &= \hat{C}_{11} - \frac{\hat{C}_{12}^2}{\hat{C}_{22}} \\
\hat{Q}_{12} &= \hat{C}_{12}\left(1 - \frac{\hat{C}_{23}}{\hat{C}_{22}}\right) \\
\hat{Q}_{22} &= \hat{C}_{22} - \frac{\hat{C}_{23}^2}{\hat{C}_{22}} \\
\hat{Q}_{66} &= \hat{C}_{66}
\end{aligned} \tag{6}$$

where the reduced relaxation matrix $[\hat{Q}]$ is symmetric. The final constitutive relationship for a unidirectional layer is given by

$$\begin{Bmatrix} \hat{\sigma}_1 \\ \hat{\sigma}_2 \\ \hat{\sigma}_6 \end{Bmatrix} = \begin{bmatrix} \hat{Q}_{11} & \hat{Q}_{12} & 0 \\ & \hat{Q}_{22} & 0 \\ \text{sym.} & & \hat{Q}_{66} \end{bmatrix} \begin{Bmatrix} \hat{\varepsilon}_1 \\ \hat{\varepsilon}_2 \\ \hat{\gamma}_6/2 \end{Bmatrix} \tag{7}$$

Equation (7) can be rotated from the material coordinate system (1,2,6) to any other coordinate orientation using the classical transformation equations of classical lamination theory. The transformation matrix for a rotation θ is

$$[T]^{-1} = \begin{bmatrix} \cos^2\theta & \sin^2\theta & -2\sin\theta\cos\theta \\ \sin^2\theta & \cos^2\theta & 2\sin\theta\cos\theta \\ \sin\theta\cos\theta & -\sin\theta\cos\theta & \cos^2\theta - \sin^2\theta \end{bmatrix} \tag{8}$$

For a layer reinforced with randomly oriented fibers (such as continuous strand mat, chopped strand mat, etc.) we propose the following reduced relaxation matrix

$$\hat{Q}^{CSM} = \frac{1}{\pi}\int_0^{\pi} [T]^{-1}[\hat{Q}][T]^{-T} \, d\theta \tag{9}$$

After completing the integral, the coefficients of the matrix are given by

$$\begin{aligned}
\hat{Q}_{11}^{CSM} &= \hat{Q}_{22}^{CSM} = \frac{3}{8}\hat{Q}_{11} + \frac{1}{4}\hat{Q}_{12} + \frac{3}{8}\hat{Q}_{22} + \frac{1}{2}\hat{Q}_{66} \\
\hat{Q}_{12}^{CSM} &= \hat{Q}_{21}^{CSM} = \frac{1}{8}\hat{Q}_{11} + \frac{3}{4}\hat{Q}_{12} + \frac{1}{8}\hat{Q}_{22} - \frac{1}{2}\hat{Q}_{66} \\
\hat{Q}_{66}^{CSM} &= \frac{1}{8}\hat{Q}_{11} - \frac{1}{4}\hat{Q}_{12} + \frac{1}{8}\hat{Q}_{22} + \frac{1}{2}\hat{Q}_{66} \\
\hat{Q}_{16}^{CSM} &= \hat{Q}_{26}^{CSM} = 0
\end{aligned} \tag{10}$$

Next, a laminated composite material can be represented by applying classical lamination theory, but in the Carson domain. If the laminate is symmetric about the midplace surface, the relation between the stress resultants and strains is

$$\begin{Bmatrix} \hat{N}_x \\ \hat{N}_y \\ \hat{N}_{xy} \end{Bmatrix} = \begin{bmatrix} \hat{A}_{11} & \hat{A}_{12} & 0 \\ & \hat{A}_{22} & 0 \\ \text{sym.} & & \hat{A}_{66} \end{bmatrix} \begin{Bmatrix} \hat{\varepsilon}_x \\ \hat{\varepsilon}_y \\ \hat{\gamma}_{xy} \end{Bmatrix} \tag{11}$$

with

$$\hat{A}_{ij} = \sum_{k=1}^{n} \hat{Q}_{ij}^{(k)} t^{(k)} \tag{12}$$

where the superscript (k) indicates the layer number, $t^{(k)}$ is the layer thickness and n is the number of layers.

Following the theory presented in Sections 2 and 3, a computer program was written to perform the micro/macro-mechanical analysis. The basis for the program is micro-mechanics [Equation (1)] and classical lamination theory [Equation (11)]. The program uses a numerical collocation method developed by Bellman [6] to perform the inverse Laplace transform of the relaxation matrix $[\hat{A}]$ matrix [Equation (11)]. The numerical inversion technique provides the solution at N points. An additional solution point at $t = 0$ is obtained using the initial value theorem

$$[A(t = 0)] = \lim_{s\to\infty} [\hat{A}(s)]$$

or simply by computing the elastic stiffness matrix $[A(t = 0)]$. The $N + 1$ points are then fitted with the same empirical model used to represent the matrix creep data in the time domain (Maxwell, power law, etc.).

Working in the Carson domain, the relaxation matrix $[\hat{A}]$ was inverted analytically to obtain the creep compliance matrix

$$[\hat{\alpha}] = [\hat{A}]^{-1}$$

which can be back-transformed to the time domain using the same procedure described above. The collection method provides N points for each coefficient of the creep compliance matrix $[\alpha(t)]$ ($N = 5$ was used in the examples).

An additional point can be obtained by using the initial value theorem or simply by computing the elastic compliance of the laminate $[\alpha(t = 0)]$. The $N + 1$ points can be fitted with the same empirical model used to fit the matrix creep data (the Maxwell model was used in the examples).

4. REPRESENTATION OF CREEP DATA

A simple method for representing the relaxation and compliance moduli of the matrix and the composite is needed for structural design. The simplest method of representation is by a spring and dashpot system where the spring represents the initial response of the material and the dashpot represents the time dependence property of the material [8]. The time dependent property displays the viscous damping of the material over time. Any arrangement of a spring-dashpot system can be used to describe the response of a material, but the most common representation used in engineering design is the Maxwell 2-parameter model. The Maxwell model has two parameters, the initial modified compliance $1/K$ and the creep rate $1/C$. The Maxwell model can be illustrated as a single series spring-dashpot system, as shown in Figure 1. The mathematical representation is given by

$$\frac{\varepsilon(t)}{\sigma_0} = \frac{1}{K} + \frac{t}{C} \tag{13}$$

where σ_0 is the applied constant stress. A graphical representation is given by Figure 2.

The initial modified compliance $1/K$ of the Maxwell model is not the inverse of the elastic modulus of the material, as shown in Figure 2. The graph shows that the Maxwell model does not fit well the primary creep region, but represents well the secondary creep region. Accurate modeling of the primary creep region is often not necesary in structural design because these effects occur over a short period of time compared to the service life of the structure. The pa-

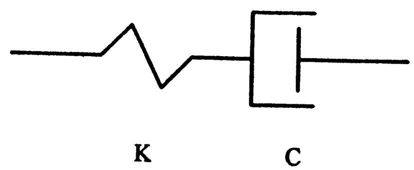

Figure 1. Maxwell spring-dashpot system.

rameter $1/C$ is the creep rate of the material. This model has been primarily used to describe metallic materials which display straight line secondary creep regions over very long periods of time. The use of this model to represent the response of polymer materials has been controversial, because a power law better represents the creep of polymers for relatively short times. For structural design, however, the main interest is on the response for long periods of time. Experimental data for both neat matrix and composites suggest that the Maxwell model provides a good representation for long times. Because of its simplicity compared to the power law, the Maxwell model is routinely used in design. The Maxwell-Voigt 4-parameter model can be used if the primary creep region needs to be modelled accurately. For long values of time, the 4-parameter model reduces to the 2-parameter model.

5. EXPERIMENTAL SETUP

Two different laminated composites were chosen for the experimental program. The constituents of each laminate are described in Table 1. The constituent properties of the reinforcing fabrics are described in Table 2, which provides the amount

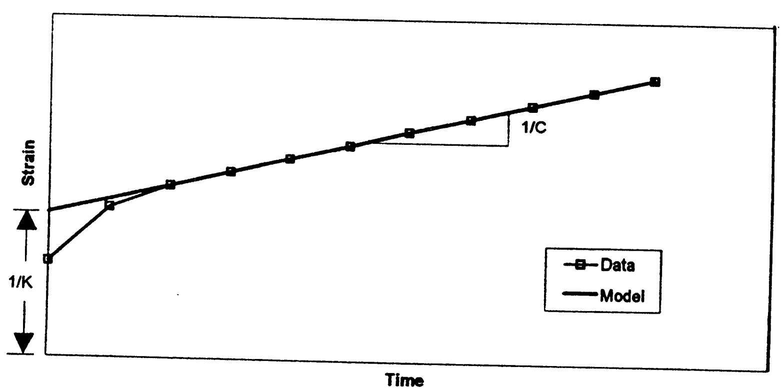

Figure 2. Graphical representation of the Maxwell model.

Table 1. Laminate constituents.

Laminate	Resin	Fiber	Fiber Volume Fraction (v_f)	Nominal Thickness (mm)
$[(90/CSM)_4]_s$	Derakane 411-350	BTI UM1810	68%	4.115
$[(90/+45/-45/CSM)_3]_s$	Derakane 411-350	BTI TVM3408	44%	7.087

of fiber in each direction of the laminated composites. The laminates were fabricated using vacuum assisted resin transfer molding (VARTM), also known as SCRIMP. The matrix was Derakane 411-350 with cumene hydroperoxide (CHP) used as a catalyst and cobalt naphthenate (CoNap) used as a promoter.

A method for testing the creep response of materials at a constant load is accomplished by using a dead load testing machine, allowing the specimen to be loaded up to 53.4 kN. The grips are constructed out of 7075-T6 aluminum which displays negligible corrosive effects in the environmental chamber. The method of fastening the specimens to the grips is by using pins which allows for thermal expansion of the system and for the specimen to be aligned properly.The specimen, shown in Figure 3, is dog-boned to ensure that the maximum creep region will be in the center of the specimen. The dimensions were selected to prevent creep or failure at the grip region for the neat matrix samples. The composite specimens were fabricated with the same dimensions, which provided more than sufficient strength in the grip region.

An environmental chamber, Cincinnati Sub Zero ZH-32, enclosed the sample and the grips. The chamber has a temperature range of –40°F to 375°F and a humidity range of 0% RH to 99% RH. The chamber is digitally controlled and can be programmed for constant or transient conditions. The strain over time was measured by strain gage mounted on the sample. A Micro Measurements CEA-13-250UN-120 strain gage was used. This strain gage has a temperature range of –100°F to 400°F for continuous use in static measurements and has a strain limit of 5%. Micro Measurements M-bond 200 adhesive is used to fasten the gage to the specimens which is allowable to be used within the temperature limits of the tests. To keep the strain gage protected from the hot and wet environment, an RTV coating was applied over the gage area (Figure 3). The RTV coating used is Dow Corning 3140 RTV which is non-corrosive and will not damage the strain gage. Standard strain

Table 2. Fiber fabric properties.

Fiber Mat	90° (oz/yd^2)	+45° (oz/yd^2)	–45° (oz/yd^2)	CSM (oz/ft^2)
BTI UM1810	18	—	—	1.0
BTI TVM3408	16	9	9	0.75

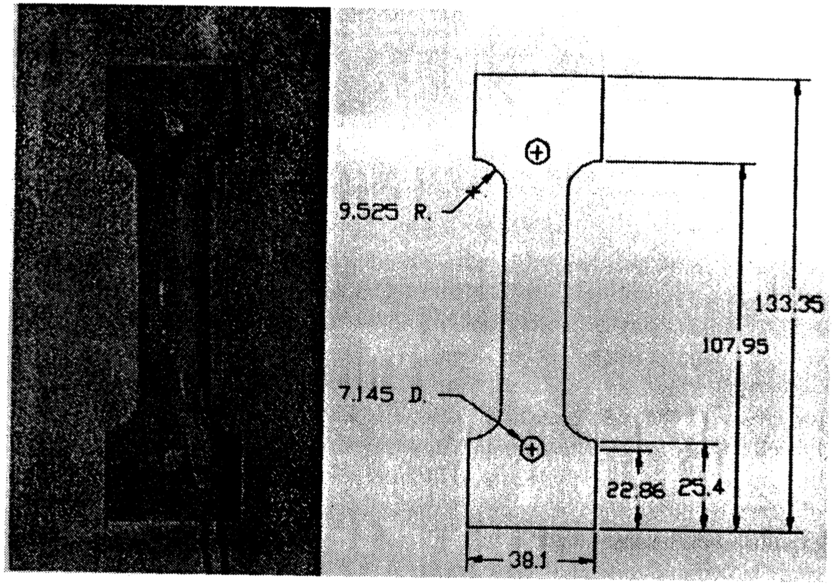

Figure 3. *Creep specimen.*

gage application techniques are used to fasten the gages. The strain gage was wired for temperature compensation. Finally, the method of applying the load to the specimen is accomplished by using a crank mechanism. This method allows for the load to be applied instantaneously to the specimen.

The strength and elastic modulus were determined separately by a quasi-static test in a universal testing system. During creep testing, the stress level should be within the linearly elastic range of the stress-strain response, which is known from the previous quasi-static tests. The tests were run until a well-defined secondary creep region developed. A time period of four hours proved to be sufficient for all temperature and humidity conditions included in the experimental program.

6. EXPERIMENTAL RESULTS

Experimental creep tests were performed on the polymer matrix and on the two previously described laminates. The matrix was the first material to be tested and evaluated. The material was tested at a constant stress level approximately one quarter of the ultimate strength (11 MPa). The low stress level was chosen to display that the material has a significant creep response even at low stress levels. The tests were condicted for a period of four hours, which is suffi-

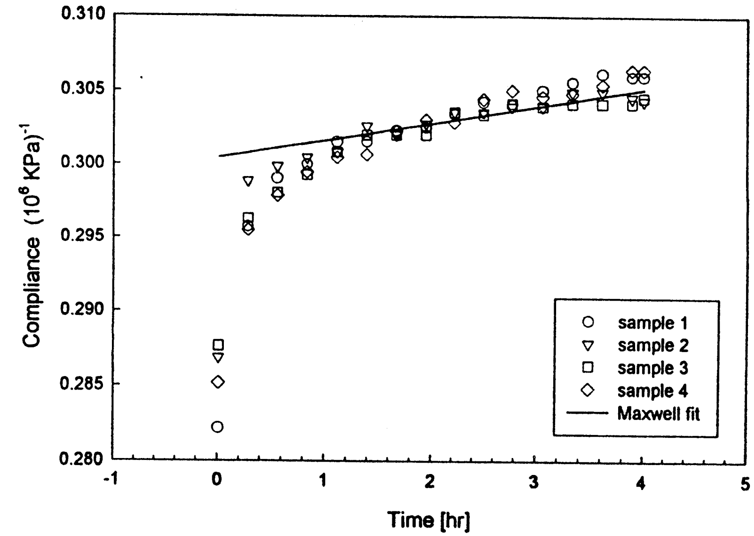

Figure 4. *Comparison on predicted and observed response for matrix at 70°F and 12% ambient RH.*

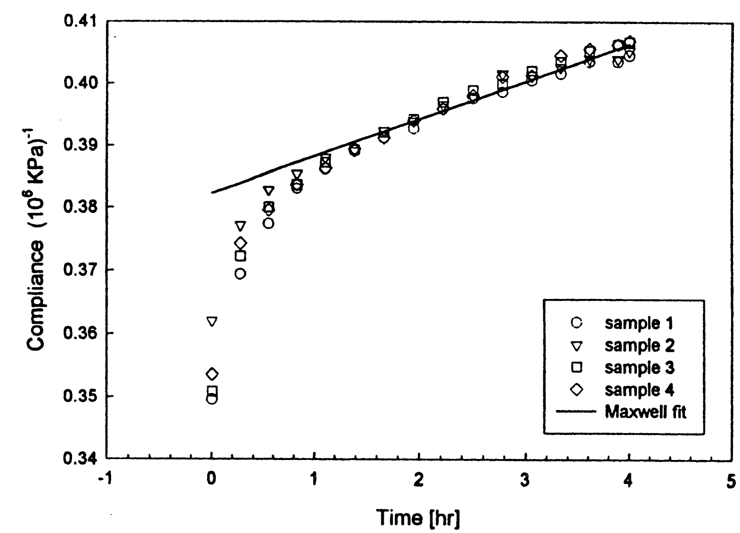

Figure 5. *Comparison on predicted and observed response for matrix at 150°F and 80% ambient RH.*

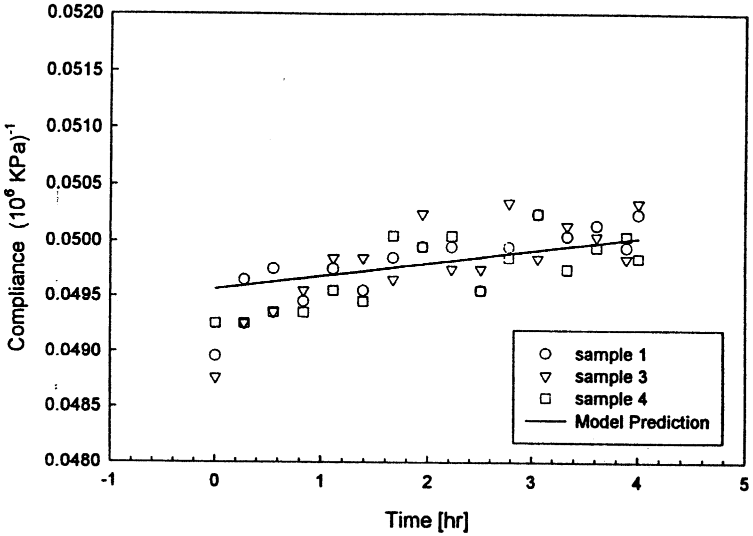

Figure 6. *Comparison on predicted and observed response for* $[(90/CSM)_4]_s$ *at 70°F and 12% ambient RH.*

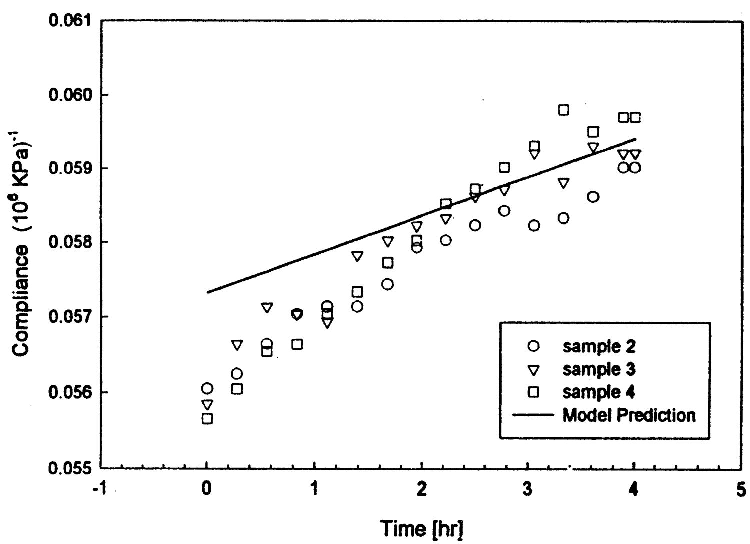

Figure 7. *Comparison on predicted and observed response for* $[(90/CSM)_4]_s$ *at 150°F and 80% ambient RH.*

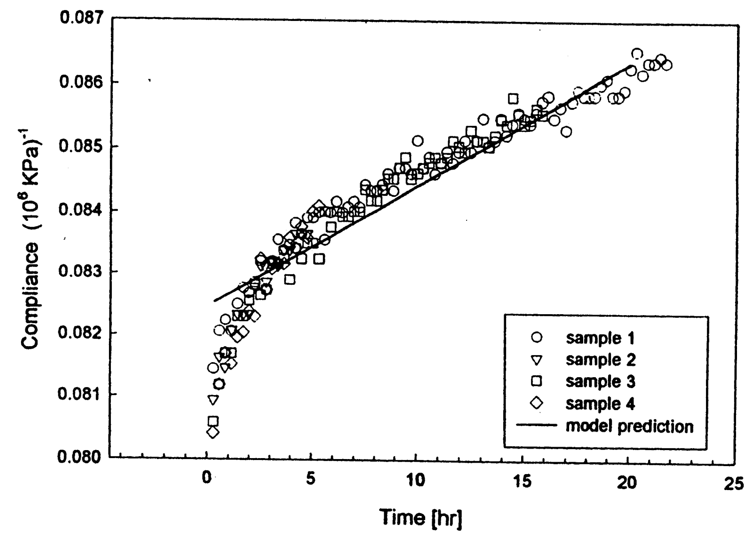

Figure 8. *Comparison on predicted and observed response for* $[(90/\pm 45/CSM)_3]_s$ *at 70°F and 12% ambient RH.*

cient to display the primary and secondary regions of the material quite well. Two sets of four specimens were tested at two different environmental conditions. The measured creep response of the matrix is shown in Figures 4–5. The creep strain rate increases with temperature and humidity, as expected [21]. Also, the primary crep region extends over a longer time as a result of increased temperature and humidity, but a clearly defined secondary creep region is observed within the first four hours of testing.

The creep response of the $[(90/CSM)_4]_s$ and $[(90/+45/-45/CSM)_3]_s$ laminates have the same general trends as the neat vinyl ester matrix, with two exceptions; the initial strain of the laminates is lower in value compared to the matrix, and the secondary creep rates of the laminates are lower in value compared to the matrix, as expected. These laminates were tested for four to twenty hours at approximately one quarter of the ultimate strength of each laminate (9 MPa and 29.6 MPa respectively). The creep response of these materials is illustrated in Figures 6–8.

7. MODELING PREDICTIONS

The Maxwell model was used to describe matrix creep data. The data in Figures 4–5 are converted into compliance dividing it by the constant applied stress σ_0. Then, a linear regression is performed using Equation (13) to obtain the parameters

Table 3. Maxwell fit parameters for the matrix at each environmental condition.

Environment	K (10^6 kPa)	C (10^6 kPa*hr)
21.1°C and 12% RH	3.328	854.6
65.6°C and 80% RH	2.616	165.9

Table 4. Maxwell fit parameters for $[(90/CSM)_4]_s$ at each environmental condition.

Environment	K (10^6 kPa)	C (10^6 kPa*hr)
21.1°C and 12% RH	20.17	8566.5
65.6°C and 80% RH	17.45	1910.2

Table 5. Maxwell fit parameters $[(90/+45/-45/CSM)_3]_s$ at each environmental condition.

Environment	K (10^6 kPa)	C (10^6 kPa*hr)
21.1°C and 12% RH	12.12	5146.3
65.6°C and 80% RH	10.71	1180.8

given in Table 3, for the matrix at the two environmental conditions. The quality of the approximation achieved with the Maxwell fit is illustrated in Tables 4–5.

The first stage of the laminate modeling was to predict the creep response of the $[(90/CSM)_4]_s$ laminate which is most susceptible to creep, because the fiber orientation is transverse to the loading direction. The micro/macro-mechanical model developed in Sections 2 and 3 predicts the secondary creep response of the composite experimental data with good agreement (Figures 6–7). The second laminate to be modeled was the $[(90/+45/-45/CSM)_3]_s$ composite (Figure 8). In both environmental conditions, the micro/macro-mechanical model predicts the secondary creep response with good agreement. Tests were performed for 20 hours on the $[(90/+45/-45/CSM)_3]_s$ laminate to validate the model predictions for periods of time longer than those used to collect matrix creep data.

Comparisons between the experimental data and values predicted using the proposed model (Sections 2 and 3) are shown in Figures 6–8. The predictions were obtained using the four-hour matrix creep response properties to predict the creep response of the laminate for up to twenty hours (see Figure 8). It can be seen that the model is able to predict the response of the composite accurately. The model predicts all the components of the compliance and relaxation including shear and transverse properties. Only the component of the compliance corresponding to the available experimental data is shown in the figures.

8. CONCLUSIONS

A new micro/macro-mechanical model was developed to predict the linear viscoelastic behavior of laminated composites, which may include random and fabric reinforcement. The method requires only experimental creep data for the matrix. The creep properties of the composite are obtained using micromechanics and macro-mechanics in the Laplace domain, followed by a backtransformation to the time domain. As such, the method is restricted to linearly viscoelastic materials.

Experimental creep data is presented and used to validate the model. Within the scope of this investigation, good agreement was achieved between the experimental data of the $[(90/CSM)_4]_s$ and the $[(90/+45/-45/CSM)_3]_s$ laminates and the proposed model at short and long time response, even when the matrix creep behavior was experimentally characterized only for a short time. The Maxwell model was used to represent the matrix creep data, and also to display the predicted composite creep behavior. However, any model such as Maxwell-Voigt or power law, can be used following the same procedure [10].

ACKNOWLEDGEMENTS

The support provided by the West Virginia Department of Transportation Division of Highways under contract SPN T-699-PTP/BD-1 is gratefully acknowledged. The participation of M. Puckett from Dow Chemicals and K. Bernetich from HardCore DuPont is greatly appreciated.

REFERENCES

1. Aboudi, J. 1982. "A Continuum Theory of Fiber-Reinforced Elastic-Viscoplastic Composites," *Int. J. Engr. Sci.*, 20:605–621.
2. Aboudi, J. 1986. "Elastoplasticity Theory for Composite Materials," *Solid Mechanics Archives*, 11:141–183.
3. Aboudi, J. 1991. *Mechanics of Composite Materials*. Amsterdam: Elsevier Science Publishers, pp. 124–154.
4. Agarwal, B. D. and L. J. Broutman. 1990. *Analysis and Performance of Fiber Composites*, New York: John Wiley and Sons, Inc.
5. Barbero, E. J. and R. Luciano. 1995. "Micromechanical Formulas for the Relaxation Tensors of Linear Viscoelastic Composites with Transversely Isotropic Fibers," *International Journal of Solids and Structures*, 32(13):1859–1872.
6. Bellman, R. 1966. *Numerical Inversion of the Laplace Transform*, New York: Elsevier.
7. Dillard, D. A., D. H. Morris and H. F. Brinson. 1981. "Creep and Creep-Rupture of Laminated Graphite-Epoxy Composites," VPI&SU Report VPI-E-81-3, Blacksburg, VA.
8. Flugge, W. 1967. *Viscoelasticity*, Waltham, MA: Blaisdell Publishing Company.
9. Puckett, M. Private communication.
10. Harris, J. 1996. "Environmental Effects on the Creep Response of Polymer Matrix Composites and Metal Matrix Composites," M.S. thesis, West Virginia University, WV.
11. Halpin, J. C. and D. F. Sims. 1974. "Methods for Determining the Elastic and Viscoelastic Response of Composite Materials," *Composite Materials: Testing and Design (Third Conference)*, pp. 46–66.
12. Jones, R. M. 1975. *Mechanics of Composite Materials*, Bristol, PA: Taylor & Francis.
13. Kennedy, T. C. and M. Wang. 1994. "Three-Dimensional, Nonlinear Viscoelastic Anaslysis of Laminated Composites," *Journal of Composite Materials*, 28:902–923.
14. Lee, O-C. and C. E. S. Ueng. 1995. "Creep Phenomenon of Simple Composite Structures," *J. Composite Materials*, 29(15):2069–2089.
15. Lin, K. Y. and I. H. Hwang. 1989. "Thermo-Viscoelastic Analysis of Composite Materials," *Journal of Composite Materials*, 23:554–569.
16. Lou, Y. C. and R. A. Schapery. 1971. "Viscoelastic Characterization of a Fiber Reinforced Plastic," *J. Composite Materials*, 5(4):208–234.
17. Luciano, R. and E. J. Barnero. 1994. "Formulas for the Stiffness of Composites with Periodic Microstructure," *International Journal of Solids and Structures*, 31(21):2933–2944.
18. Luciano, R. and Barbero, E. J. 1995. "Analytical Expressions for the Relaxation Moduli of Linear Viscoelastic Composites with Periodic Microstructure," *ASME Journal of Applied Mechanics*, 62(3):786–793.
19. Schapery, R. A. 1967. "Stress Analysis of Viscoelastic Composite Materials," *Journal of Composite Materials*, 1:228–267.
20. Schapery, R. A. 1974. "Viscoelastic Behavior and Analysis of Composites Materials," in *Mechanics of Composite Materials, Vol. 2*, G. P. Sendeckyj, ed., New York: Academic Press.
21. Shen, C. H. and G. S. Springer. 1981. "Effects of Moisture and Temperature on the Tensile Strength of Composite Materials," in *Environmental Effects on Composite Materials, Vol. 1*, G. S. Springer, ed., Lancaster, PA: Technomic Publishing Co., Inc.

22. Singhal, S. N. and C. C. Chamis. 1992. "Environmental Defects on Long Term Behavior of Composite Laminates," *24th International SAMPE Technical Conference*, October 20–22.
23. Tuttle, M. E. and H. F. Brinson. 1985. "Prediction of the Long-Term Creep Compliance of General Composite Laminates," *Experimental Mechanics*, 89–102.
24. Yancey, R. N. and M. J. Pindera. 1990. "Micromechanical Analysis of the Creep Response of Unidirectional Composites," *ASME Journal of Engineering Materials and Technology*, 112:157–163.
25. Walrath, D. E. 1989. "Viscoelastic Response of a Unidirectional Composite Containing Two Viscoelastic Constituents," *Experimental Mechanics*, 111–117.
26. Zhang, S. Y. and Xiang, X. Y. 1992. "Creep Characterization of a Fiber Reinforced Plastic Material," *Journal of Reinforced Plastics and Composites*, 2:1187–1194.